Magnetic Phase Transitions in One-Dimensional Strongly Attractive Three-Component Ultracold Fermions

X. W. Guan,[1] M. T. Batchelor,[1,2] C. Lee,[3] and H.-Q. Zhou[4]

[1]*Department of Theoretical Physics, Research School of Physical Sciences and Engineering, Australian National University, Canberra ACT 0200, Australia*

[2]*Mathematical Sciences Institute, Australian National University, Canberra ACT 0200, Australia*

[3]*Nonlinear Physics Centre and ARC Centre of Excellence for Quantum-Atom Optics, Research School of Physical Sciences and Engineering, Australian National University, Canberra ACT 0200, Australia*

[4]*Centre for Modern Physics, Chongqing University, Chongqing 400044, People's Republic of China*

(Received 5 September 2007; revised manuscript received 23 December 2007; published 19 May 2008)

We investigate the nature of trions, pairing, and quantum phase transitions in one-dimensional strongly attractive three-component ultracold fermions in external fields. Exact results for the ground-state energy, critical fields, magnetization and phase diagrams are obtained analytically from the Bethe ansatz solutions. Driven by Zeeman splitting, the system shows exotic phases of trions, bound pairs, a normal Fermi liquid, and four mixtures of these states. Particularly, a smooth phase transition from a trionic phase into a pairing phase occurs as the highest hyperfine level separates from the two lower energy levels. In contrast, there is a smooth phase transition from the trionic phase into a normal Fermi liquid as the lowest level separates from the two higher levels.

DOI: 10.1103/PhysRevLett.100.200401 PACS numbers: 05.30.Fk, 02.30.Ik, 03.75.Hh, 03.75.Ss

There is considerable interest in three-component ultracold fermions [1–4]. Atomic Fermi gases with internal degrees of freedom are tunable interacting many-body systems featuring novel and subtle quantum phase transitions. Two-component Fermi gases of ultracold atoms with population imbalance have been experimentally observed to undergo a quantum phase transition between the normal and superfluid states [5]. The bound pairs form a Bardeen-Cooper-Schrieffer (BCS) superfluid, while the unpaired fermions remain as a separated normal Fermi liquid (FL). These exotic phases have revived interest in the one-dimensional (1D) integrable model of two-component fermions, which captures the physics involved in quantum phase transitions and magnetic ordering [6–9].

Three-component fermions reveal more exotic features [1–4,10–13]. The scattering lengths between atoms in different low sublevels are again tunable via Feshbach resonances [14–16]. As a consequence, BCS pairing can be favored by anisotropies in three different ways: specifically, atoms in three low sublevels denoted by $|1\rangle$, $|2\rangle$, and $|3\rangle$ can form the three possible pairs $|1\rangle + |2\rangle$, $|2\rangle + |3\rangle$, and $|1\rangle + |3\rangle$ [14]. One may also have three internal spin states exhibiting $SU(3)$ symmetry via tuning three scattering lengths close to each other [17]. Significantly, strongly attractive three-component atomic fermions can form spin-neutral three-body bound states called *trions*. Thus, a phase transition is expected to occur between pairing superfluid and trionic states [1,3,4,11].

In this Letter, we consider 1D three-component ultracold fermions with δ-function interaction in external magnetic fields. Although this model was solved long ago by the Bethe ansatz (BA) [18,19], its physics is far from being thoroughly understood. Here we study the precise nature of trions and pairing in this model, and calculate critical fields and full phase diagrams by solving the BA equations and related dressed energy equations. Our analytical results for magnetism and magnetic-field-driven quantum phase transitions in attractive fermions should provide benchmarks for experiments with ultracold Fermi atoms with multiple internal states.

The model.—The Hamiltonian [18] we consider,

$$H = -\frac{\hbar^2}{2m}\sum_{i=1}^{N}\frac{\partial^2}{\partial x_i^2} + g_{1D}\sum_{1\le i<j\le N}\delta(x_i - x_j) + \sum_{i=1}^{3} N^i \epsilon_Z^i(\mu_B^i, B), \tag{1}$$

describes N fermions of mass m and spin-independent s-wave scattering lengths, which can occupy three possible hyperfine levels ($|1\rangle$, $|2\rangle$, and $|3\rangle$) and are constrained to a line of length L with periodic boundary conditions. The last term denotes the Zeeman energy, where N^i is the number of fermions in state $|i\rangle$ with Zeeman energy ϵ_Z^i determined by the magnetic moments μ_B^i and the magnetic field B. The Zeeman energy term can also be expressed as $-H_1(N^1 - N^2) - H_2(N^2 - N^3) + N\bar{\epsilon}$, where the unequally spaced Zeeman splitting in three hyperfine levels can be characterized by two independent parameters $H_1 = \bar{\epsilon} - \epsilon_Z^1(\mu_B^1, B)$ and $H_2 = \epsilon_Z^3(\mu_B^3, B) - \bar{\epsilon}$, with $\bar{\epsilon} = \sum_{\sigma=1}^{3}\epsilon_Z^{\sigma}(\mu_B^i, B)/3$ the average Zeeman energy.

In general, the scattering lengths depend on spin states. However, it is plausible to tune three scattering lengths close to each other utilizing the broad Feshbach resonances [14,20]. Thus the difference in effective interaction parameters becomes negligible so that three low spin states may have $SU(3)$ degeneracy. The coupling constant $g_{1D} = -\hbar^2 c/m$ with interaction strength $c = -2/a_{1D}$ is determined by the effective 1D scattering length a_{1D} [21]. For simplicity, we define a dimensionless interaction strength $\gamma = c/n$ with density $n = N/L$.

The energy eigenspectrum is given in terms of the quasimomenta $\{k_i\}$ of the fermions via $E = \frac{\hbar^2}{2m}\sum_{j=1}^{N} k_j^2$, which in terms of the function $e_n(x) = (x + inc/2)/(x - inc/2)$ satisfy the nested BA equations [18,19]

$$\exp(ik_jL) = \prod_{\ell=1}^{M_1} e_1(k_j - \Lambda_\ell),$$

$$\prod_{\ell=1}^{N} e_1(\Lambda_\alpha - k_\ell) = -\prod_{\beta=1}^{M_1} e_2(\Lambda_\alpha - \Lambda_\beta)\prod_{\ell=1}^{M_2} e_{-1}(\Lambda_\alpha - \lambda_\ell),$$

$$\prod_{\ell=1}^{M_1} e_1(\lambda_m - \Lambda_\ell) = -\prod_{\ell=1}^{M_2} e_2(\lambda_m - \lambda_\ell). \quad (2)$$

Here $j = 1, \ldots, N$, $\alpha = 1, \ldots, M_1$, $m = 1, \ldots, M_2$, with quantum numbers $M_1 = N^2 + N^3$ and $M_2 = N^3$. The parameters $\{\Lambda_\alpha, \lambda_m\}$ are the rapidities for the internal hyperfine spin degrees of freedom. For the irreducible representation $[3^{N_3}2^{N_2}1^{N_1}]$ three-column Young tableau encode the numbers of unpaired fermions, bound pairs and trions are given by $N_1 = N^1 - N^2$, $N_2 = N^2 - N^3$, and $N_3 = N^3$, respectively.

Trions and pairing.—In principle, different numbers of trions, pairs, and unpaired fermions can be selected to populate the ground state by carefully tuning H_1 and H_2. For a state with arbitrary spin polarization, i.e., N^i with $i = 1, 2, 3$ arbitrary, there are [19] (i) N_3 spin-neutral trions in the quasimomentum k space accompanied by N_3 spin bound states in the Λ-parameter space and N_3 real roots in the λ-parameter space, (ii) N_2 BCS bound pairs in k space accompanied by N_2 real roots in Λ space, and (iii) N_1 unpaired fermions in k space. With the above configuration, we solve the BA equations (2) in the strong coupling regime $L|c| \gg 1$ to give the quasimomenta for trions, BCS pairs, and unpaired fermions (see Fig. 1), from which the energy is given by

$$\frac{E}{L} \approx \frac{\hbar^2}{2m}\left[\frac{\pi^2 n_1^3}{3}\left(1 + \frac{8n_2 + 4n_3}{|c|}\right) - \frac{n_2c^2}{2} + \frac{\pi^2 n_2^3}{6}\left(1 + \frac{12n_1 + 6n_2 + 16n_3}{3|c|}\right) - 2n_3c^2 + \frac{\pi^2 n_3^3}{9}\left(1 + \frac{12n_1 + 32n_2 + 18n_3}{9|c|}\right)\right]. \quad (3)$$

Here $n_a = N_a/L$, with $a = 1, 2, 3$ the density for unpaired fermions, pairs, and trions, respectively. This state can be viewed as a mixture of trionic fermions, hard-core bosons, and unpaired fermions, which behave essentially like particles with different statistical signatures [2,8]. The BCS pair binding energy $\epsilon_b = \hbar^2c^2/(4m)$ and the binding energy $\epsilon_t = \hbar^2c^2/m$ for a trion can be read off Eq. (3). The

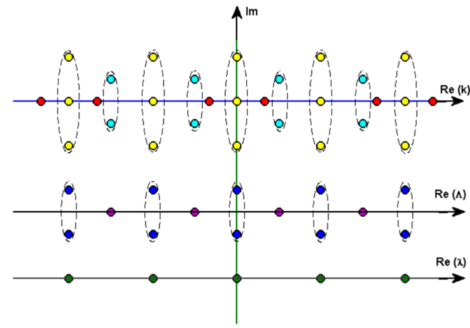

FIG. 1 (color online). Schematic configuration of Bethe ansatz quasimomenta k, spin momenta Λ and λ in the complex plane ($N = 29$ with $N_1 = 6$, $N_2 = 4$, and $N_3 = 5$) at zero temperature. For strongly attractive interaction, the unpaired and paired quasimomenta can penetrate into the central region occupied by tightly bound trions.

root patterns obtained from (2) reveal an important signature, namely, unpaired fermions couple to two different kinds—trionic and BCS pairing—of FL.

Thermodynamic Bethe ansatz.—In the thermodynamic limit, i.e., $L, N \to \infty$ with N/L finite, the grand partition function is $Z = \mathrm{Tr}(e^{-\mathcal{H}/\mathcal{T}}) = e^{-G/T}$, where the Gibbs free energy is $G = E + E_Z - \mu N - TS$ in terms of the Zeeman energy E_Z, chemical potential μ, and entropy S [22–24]. For finite temperatures, besides complex BA roots for trions, BCS pairs, and real roots for unpaired fermions, the quasimomenta $\{\Lambda_\alpha, \lambda_m\}$ form complex strings. The Gibbs free energy can be given in terms of the densities of particles and holes for trions, bound pairs, and unpaired fermions as well as spin degrees of freedom, which are determined from BA (2). Thus the true physical state is determined by the minimization of the Gibbs free energy with respect to these densities, which gives rise to a set of coupled nonlinear integral equations—the thermodynamic Bethe ansatz (TBA) equations [25].

Quantum phase transitions in the model may be analyzed via the dressed energy equations,

$$\epsilon^{(3)}(\lambda) = 3\lambda^2 - 2c^2 - 3\mu - a_2 * \epsilon^{(1)}(\lambda) - [a_1 + a_3] * \epsilon^{(2)}(\lambda) - [a_2 + a_4] * \epsilon^{(3)}(\lambda),$$

$$\epsilon^{(2)}(\Lambda) = 2\Lambda^2 - 2\mu - \frac{c^2}{2} - H_2 - a_1 * \epsilon^{(1)}(\Lambda) - a_2 * \epsilon^2(\Lambda) - [a_1 + a_3] * \epsilon^{(3)}(\Lambda),$$

$$\epsilon^{(1)}(k) = k^2 - \mu - H_1 - a_1 * \epsilon^{(2)}(k) - a_2 * \epsilon^{(3)}(k), \quad (4)$$

which follow from the TBA equations in the limit $T \to 0$. Here the function $a_j(x) = \frac{1}{2\pi}\frac{j|c|}{(jc/2)^2 + x^2}$ and $\epsilon^{(a)}$ are the dressed energies; $a_j * \epsilon^{(a)}(x) = \int_{-Q_a}^{+Q_a} a_j(x - y)\epsilon^{(a)}(y)dy$ is the convolution. The negative part of the dressed energies $\epsilon^{(a)}(x)$ for $x \le |Q_a|$ corresponds to the occupied states in the Fermi seas of trions, bound pairs, and unpaired fermions, with the positive part of $\epsilon^{(a)}$ corresponding to the unoccupied states. The integration boundaries Q_a characterize the "Fermi surfaces" at $\epsilon^{(a)}(\pm Q_a) = 0$. The zero-temperature Gibbs free energy per unit length is given by $G = \sum_{a=1}^{3} \frac{a}{2\pi} \int_{-Q_a}^{+Q_a} \epsilon^{(a)}(x)dx$. The chemical potential and magnetization per length are determined by H_1, H_2, g_{1D}, and n through the relations

$$-\frac{\partial G}{\partial \mu} = n, \qquad -\frac{\partial G}{\partial H_1} = n_1, \qquad -\frac{\partial G}{\partial H_2} = n_2. \tag{5}$$

In the absence of analytic solutions of Eq. (4), we obtain an exact expansion in the strong coupling regime $\gamma \gg 1$. Solving the dressed energy equations (4) by iteration among the relations (5) and $\epsilon^a(\pm Q_a) = 0$ with $a = 1, 2, 3$, giving the effective chemical potentials

$$\begin{aligned}
\mu^t &\approx \frac{n_3^2}{9}\left(1 + \frac{4n_1}{3|c|} + \frac{32n_2}{9|c|} + \frac{8n_3}{3|c|}\right) + \frac{4n_1^3}{9|c|} + \frac{8n_2^3}{27|c|},\\
\mu^b &\approx \frac{n_2^2}{4}\left(1 + \frac{4n_1}{|c|} + \frac{8n_2}{3|c|} + \frac{16n_3}{3|c|}\right) + \frac{4n_1^3}{3|c|} + \frac{16n_3^3}{81|c|},\\
\mu^u &\approx n_1^2\left(1 + \frac{8n_2}{|c|} + \frac{4n_3}{|c|}\right) + \frac{2n_2^3}{3|c|} + \frac{4n_3^3}{27|c|}
\end{aligned} \tag{6}$$

in units of $\hbar^2\pi^2/2m$. Here we denote $\mu^t = \mu + \epsilon_t/3$ for trions, $\mu^b = \mu + \epsilon_b/2 + H_2/2$ for bound pairs, and $\mu^u = \mu + H_1$ for unpaired fermions. These results give rise to a full characterization of three Fermi surfaces. It is important to note [25] that the energy for arbitrary population imbalances can be obtained from $E/L = \mu n + G + n_1 H_1 + n_2 H_2$, which coincides with (3) derived from the discrete BA (2). This indicates that the trions and BCS bound pairs are possibly the true physical states; i.e., the BA roots comprise the equilibrium states in the thermodynamic limit.

Full phase diagram.—In the strong coupling regime and in the absence of Zeeman splitting, i.e., $H_1 = H_2 = 0$, the dressed energies $\epsilon^{(2)}$ and $\epsilon^{(1)}$ are always positive, i.e., $Q_1 = Q_2 = 0$. Thus trions form a singlet ground state. However, the Zeeman splitting can lift the $SU(3)$ degeneracy and drive the system into different phases. Breaking a trion state requires a spin excitation energy to diminish an energy gap. From Eq. (4), the energy transfer relations among the binding energy, the Zeeman energy, and the variation of chemical potentials between different Fermi seas are given by

$$\begin{aligned}
H_1 &= 2c^2/3 + (\mu^u - \mu^t),\\
H_2 &= 5c^2/6 + 2(\mu^b - \mu^t),\\
H_1 - H_2/2 &= c^2/4 + (\mu^u - \mu^b).
\end{aligned} \tag{7}$$

These equations determine the full phase diagram and the critical fields triggered by the Zeeman splitting H_1 and H_2. A similar energy transfer relation was identified in an experiment for 1D polarized two-component fermions

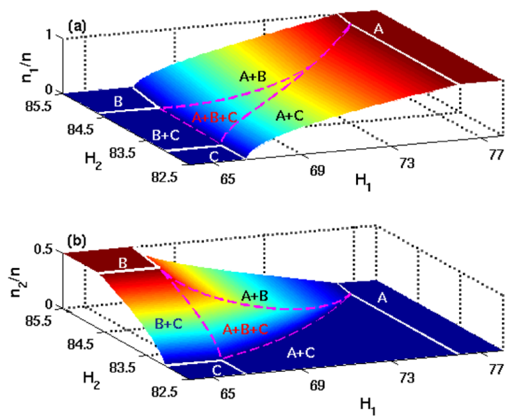

FIG. 2 (color online). Phase diagram determined by the energy transfer relations (7) with chemical potentials (6) with $|c| = 10$ and $n = 1$. Panels (a) and (b) show the polarizations n_1/n and n_2/n vs the fields H_1 and H_2. The figure reveals a novel trion phase C, a pairing phase B, an unpaired phase A, and four different mixtures of these states.

[20]. These relations hold for arbitrary interaction strength. However, for $\gamma \gg 1$, the chemical potentials are given by Eq. (6). Figure 2 shows the polarization, which clearly indicates novel magnetism, new quantum phases, multicritical points, and phase transitions in terms of Zeeman splitting.

The ground-state energy vs Zeeman splitting parameters H_1 and H_2 can be evaluated from Eq. (3) with the densities n_1 and n_2 determined from (7). Figure 3 shows the energy surface for all possible phases shown in Fig. 2. This figure demonstrates the interplay between different physical ground states. We see a mixture of trions, BCS pairs, and unpaired fermions ($A + B + C$) populates the ground state for certain values of H_1 and H_2. There are six different phase transitions across the $A + B + C$ boundaries in the

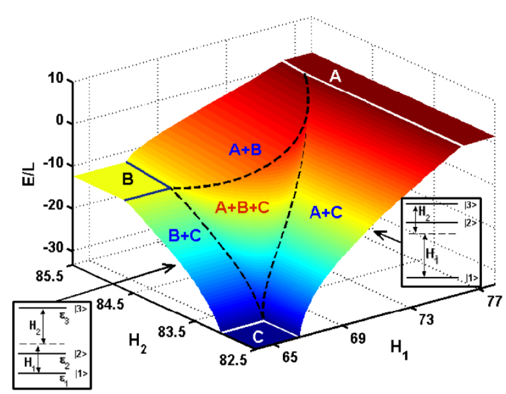

FIG. 3 (color online). Ground-state energy vs Zeeman splitting for $|c| = 10$ and $n = 1$. In the vicinity of the multicritical points and the phase boundaries, the energy surface varies continuously with H_1 and H_2. The insets indicate configurations for the cases of small H_1 and small H_2. The dashed lines in the insets indicate the average Zeeman energy $\bar{\epsilon}$.

H_1-H_2 plane. All phase transitions between two phases are second order and reveal a universality class of linear-field-dependent magnetization with finitely divergent susceptibility in the vicinities of critical fields. Our analytical results (7) do not support the square-root-field-dependent behavior of magnetization argued in [23], but do agree with results for the attractive Hubbard model [26].

For small H_1 (i.e., small splitting between the two lower levels), a smooth phase transition from a trionic state into a mixture of trions and pairs occurs as H_2 exceeds the lower critical value H_2^{c1} (see Fig. 3). When H_2 is greater than the upper critical value H_2^{c2}, the atoms within the two lower states form a pure pairing phase with $SU(2)$ symmetry and the highest level remains unpopulated. In this pure pairing phase, the three-level system is reduced to a two-level one. Trions and BCS pairs coexist when $H_2^{c1} < H_2 < H_2^{c2}$. The critical fields $H_2^{c1} \approx \frac{\hbar^2 n^2}{2m}[\frac{5\gamma^2}{6} - \frac{2\pi^2}{81}(1 + \frac{8}{27|\gamma|})]$ and $H_2^{c2} \approx \frac{\hbar^2 n^2}{2m}[\frac{5\gamma^2}{6} + \frac{\pi^2}{8}(1 + \frac{20}{27|\gamma|})]$ are uniquely determined by the second equation in (7). The polarization curve n_2/n indicates that the phase transitions in the vicinities of the critical lines H_2^{c1} and H_2^{c2} are of second order. In addition, the phase transitions $B \rightarrow A + B \rightarrow A$ induced by increasing H_1 are reminiscent of those in the two-component systems [8,26]. We see clearly that equally spaced Zeeman splitting $H_1 = H_2$ does not favor spin-dependent charge states in 1D multicomponent attractive fermions.

For small H_2 (i.e., small splitting between the two higher levels), the pairing phase is not favored and the trions are broken into unpaired fermions in the lowest level (see Fig. 3). Using the first relation in (7), we see that the trionic state with zero polarization $n_1/n = 0$ forms the ground state when the field $H < H_1^{c1}$. Here $H_1^{c1} \approx \frac{\hbar^2 n^2}{2m}[\frac{2\gamma^2}{3} - \frac{\pi^2}{81} \times (1 + \frac{4}{9|\gamma|})]$ is the lowest critical field which makes the excitation gapless. If the lowest level is widely separated from the two higher levels, i.e., $H_1 > H_1^{c2} \approx \frac{\hbar^2 n^2}{2m} \times [\frac{2\gamma^2}{3} + \pi^2(1 - \frac{4}{9|\gamma|})]$, all trions are broken and the state becomes a normal FL where all atoms occupy the lowest level. Trions and unpaired fermions coexist in the intermediate region $H_1^{c1} < H_1 < H_1^{c2}$.

For trapped systems, these exotic phases and their segments in real space can be predicted with the help of the local density approximation. For example, for small H_1, a mixture of trions and BCS pairs lies in the trap center and the fully trionic phase (or the fully pairing phase) sits in the two outer wings for $H_2 < \frac{5\hbar^2 n^2 \gamma^2}{12m}$ (or $H_2 > \frac{5\hbar^2 n^2 \gamma^2}{12m}$). In contrast, for small H_2, a mixture of trions and unpaired fermions lies in the center and the fully trionic phase (or the fully unpaired phase) sits in the two outer wings for $H < \epsilon_t/3$ (or $H > \epsilon_t/3$).

To conclude, our analytic BA and TBA results for the critical fields, quantum phase transitions, and full phase diagrams reveal the nature of spin-neutral trions and BCS pairing in three-component ultracold fermions in external fields. Particularly, we found transitions between trionic and BCS pairing phases and between trionic and normal FL phases may occur for certain types of Zeeman splitting. These exotic phases should stimulate further experimental interest in multicomponent ultracold Fermi gases with mismatched Fermi surfaces.

This work has been supported by the Australian Research Council. The authors thank N. Andrei, M. A. Cazalilla, H. Frahm, W. V. Liu, and M. Takahashi for helpful discussions. C. L. thanks Yu. S. Kivshar for support.

[1] Á. Rapp, G. Zaránd, C. Honerkamp, and W. Hofstetter, Phys. Rev. Lett. **98**, 160405 (2007); C. Honerkamp and W. Hofstetter, Phys. Rev. Lett. **92**, 170403 (2004).
[2] P. Lecheminant, E. Boulat, and P. Azaria, Phys. Rev. Lett. **95**, 240402 (2005); S. Capponi *et al.*, Phys. Rev. A **77**, 013624 (2008).
[3] R. W. Cherng, G. Refael, and E. Demler, Phys. Rev. Lett. **99**, 130406 (2007).
[4] F. Wilczek, Nature Phys. **3**, 375 (2007).
[5] M. W. Zwierlein, A. Schirotzek, C. H. Schunck, and W. Ketterle, Science **311**, 492 (2006); M. W. Zwierlein, C. H. Schunck, A. Schirotzek, and W. Ketterle, Nature (London) **442**, 54 (2006); G. B. Partridge *et al.*, Science **311**, 503 (2006).
[6] G. Orso, Phys. Rev. Lett. **98**, 070402 (2007).
[7] H. Hu, X.-J. Liu, and P. D. Drummond, Phys. Rev. Lett. **98**, 070403 (2007).
[8] X.-W. Guan, M. T. Batchelor, C. Lee, and M. Bortz, Phys. Rev. B **76**, 085120 (2007).
[9] A. E. Feiguin and F. Heidrich-Meisner, Phys. Rev. B **76**, 220508(R) (2007).
[10] T. Paananen, J.-P. Martikainen, and P. Törmä, Phys. Rev. A **73**, 053606 (2006).
[11] Á. Rapp, W. Hofstetter, and G. Zaránd, arXiv:0707.2378.
[12] H. Zhai, Phys. Rev. A **75**, 031603(R) (2007).
[13] X.-J. Liu, H. Hu, and P. D. Drummond, Phys. Rev. A **77**, 013622 (2008).
[14] M. Bartenstein *et al.*, Phys. Rev. Lett. **94**, 103201 (2005).
[15] C. A. Regal and D. S. Jin, Phys. Rev. Lett. **90**, 230404 (2003).
[16] E. R. I. Abraham *et al.*, Phys. Rev. A **55**, R3299 (1997).
[17] T. Luu and A. Schwenk, Phys. Rev. Lett. **98**, 103202 (2007).
[18] B. Sutherland, Phys. Rev. Lett. **20**, 98 (1968).
[19] M. Takahashi, Prog. Theor. Phys. **44**, 899 (1970).
[20] H. Moritz *et al.*, Phys. Rev. Lett. **94**, 210401 (2005).
[21] T. Bergeman, M. G. Moore, and M. Olshanii, Phys. Rev. Lett. **91**, 163201 (2003).
[22] M. Takahashi, *Thermodynamics of One-Dimensional Solvable Models* (Cambridge University Press, Cambridge, 1999).
[23] P. Schlottmann, Int. J. Mod. Phys. B **11**, 355 (1997).
[24] M. T. Batchelor, X.-W. Guan, N. Oelkers, and Z. Tsuboi, Adv. Phys. **56**, 465 (2007).
[25] X.-W. Guan and M. T. Batchelor (to be published).
[26] F. Woynarovich and K. Penc, Z. Phys. B **85**, 269 (1991).